

Report May 2020. Improvements to the AUF: Photometric Considerations

Tom J. Wilson and Tim Naylor

ABSTRACT

This report discusses the extensions to the WP deliverable 3.11.1 March report, in which we highlighted the need to improve the model for contamination at LSST depths from a photometry perspective. First, we derive the magnitude limit down to which simulated objects must be realised within Monte Carlo simulations to ensure that the reported photometric contamination is statistically complete. This considers the cumulative expectation number of sources within a given PSF circle down to some Δm limit, and the probability that zero sources are drawn. Limiting this to a sufficiently small fraction we can derive an acceptable perturber relative flux ratio, and show that this, along with the astrometric limit, is within the 5 magnitude limit constraint laid out previously. Second, we test the application of the new, more accurate model for astrometric perturbations to the issue of photometric contamination. Along with probabilities of cross-matches, modelled using astrometric perturbations, the composite photometric catalogues provided by the LSST:UK DAC should also provided information on the probability of relative flux brightening of sources. We therefore perform tests on the extraction and recovery of blended objects, showing that, at least qualitatively, it is reasonable to construct a completely analogous model to astrometric perturbation when describing photometric contamination.

1 INTRODUCTION

In the March report for WP deliverable 3.11.1, we discussed improvements to the description of the Astrometric Uncertainty Function (AUF) for deep, faint, background-dominated surveys and sources, crucial for ensuring that the majority of LSST objects are as accurately modelled as possible in any cross-matching process. However, when doing so, as mentioned in section 4, we only considered the *astrometric* effects; we concluded that an extension to WP3.11.1 would require a model to ensure that the *photometric* component of the Monte Carlo simulations used to model the effects of crowding were also as accurate as possible. This would then allow us to report robust statistical flux contaminations for the cross-matches reported, which would likely be of interest to some users of the resultant merged catalogue of objects.

We report here these photometric considerations. Firstly, we needed to consider the Δm limit down to which to model simulated blended objects within our Monte Carlo PSFs to ensure that we capture, in all realisations, all appropriate flux brightening within each object at the brightness of the central object. Additionally, we required further testing to understand how to handle the reporting of these flux brightenings for objects whose properties were derived with PSF-based least-squares fitting, but are not in the background-dominated regime.

However, we stress here that this work is not quite finished, as we have prioritised WP Deliverable 3.11.2 (and 3.11.3; see the six month plan April–October 2020 for more details) due to begin May/June 2020 over finishing these minor aspects of WP deliverable 3.11.1. This report provides the qualitative conclusions that will round out WP deliverable 3.11.1, as per section 4 of the March report, but will require further follow up to smooth over a few

loose threads and create the eventual implementation for the final deliverable of the project.

2 THE PHOTOMETRIC LIMIT OF THE PERTURBATION AUF

The original algorithm for deriving the additional components of the AUF – aside from the original, intrinsic, noise-based Gaussian component – used by Wilson & Naylor (2018) called for a $\Delta m = 10$ magnitude limit for the perturbation-specific aspect. In this case, this limit was a simple one, based roughly on perturbations using a flux-weighted centroid, being that of the largest “small” offset caused by this faint object. For $\Delta m = 10$ we have $f = 0.0001 - f$ being the relative flux ratio between perturber and central source – and flux-weighted perturbations at most of order 0.001”, an order of magnitude below the centroiding precision of bright *WISE* objects.

However, as discussed in the March report for WP3.11.1, we can now use a magnitude-based Δm cut, based on the *individual* signal-to-noise ratio (SNR) of an object, providing a dynamic Δm limit. As this calculation only took into account the effects on the astrometry of the bright, central object we additionally need to consider whether the Δm limit would result in a complete evaluation of the flux contamination of the objects. For this, we can turn to the number of objects simulated within a given Monte Carlo realisation of the PSF.

2.1 PSF Realisation Derivation

As described by Wilson & Naylor (2018), the simulations for creating the statistical distribution of perturbations of a bright source’s

position – and contamination of its flux – involve the drawing of objects and placing them randomly near to the primary source. We then assume that, on a statistical level, all of the flux that will affect the contamination level quoted has been simulated if we define our Δm such that essentially all simulations contain at least one perturber. To compute this, we again assume our simulations are modelled as per Wilson & Naylor (2018), in which small magnitude offsets are stepped through for secondary perturbers. In each small bin m_i to $m_i + dm$ there is a given number density of objects (either a galaxy source rate or TRILEGAL [Girardi et al. 2005] Galaxy star count rate, e.g., cf. figure 5 of Wilson & Naylor 2018), converted to an expected number of source within an area of the PSF.

From this expectation count λ_i – for the i th bin – a given source number is drawn from a Poissonian distribution. We can therefore compute the expected number of sources, and cumulative distribution function (CDF), for the total number of sources down to a given Δm , given by the convolution of each individual Poissonian distribution for each small magnitude bin. Using the notation $\sum_{i=1}^n X_i = Y$, where X_i and Y are n independent random variables and the resultant convolution distribution respectively, we get

$$\sum_{i=1}^n \text{Poisson}(\lambda_i) = \text{Poisson}\left(\sum_{i=1}^n \lambda_i\right) \equiv \text{Poisson}(\lambda), \quad (1)$$

where

$$\text{Poisson}(\lambda) = P(X = k; \lambda) = \frac{\lambda^k \exp(-\lambda)}{k!} \quad (2)$$

with k the number of objects drawn. Thus the sum of n values, drawn from Poissonian distributions is, effectively, itself a drawing from a Poissonian distribution with the expectation value the sum of each individual expectation values.

We wish to find the Δm to simulate down to – or, now, the number of small magnitude bins we need to draw from – at which we get some small fraction of realisations with zero extra sources drawn. Now we can use a Poissonian distribution with its expectation value the sum of each individual expectation value, and draw the CDF for no objects,

$$P(X \leq k; \lambda) = \frac{\Gamma([k+1], \lambda)}{[k]!} \equiv \exp(-\lambda) \sum_{i=0}^{[k]} \frac{\lambda^i}{i!}, \quad (3)$$

where $[k]$ is the “floor” of k (i.e., the largest integer no larger than k), and thus our given probability, for zero objects, is

$$P(X \leq 0; \lambda) = \Gamma(1, \lambda) \equiv \exp(-\lambda). \quad (4)$$

2.2 WISE Simulations

We need to calculate $P(X \leq 0; \lambda) = y$, where y is some small fraction, here given as $y = 0.01$ – a 1% chance of realising a PSF containing no objects. Thus, for a given source density of potential contaminating sources, we can compute the *photometric* contamination limit, shown, along with the original astrometric limit, in Figure 1. This is simply the sum of all individual magnitude bin λ_i values (the number density of objects times the bin width times the PSF area) below the m of the bright, central object until $P(X \leq 0; \lambda) \leq 0.01$. For $k = 0$ and $y = 0.01$ this simplifies slightly to asking the Δm bin at which $\lambda \geq -\ln(0.01) \approx 4.6$.

The importance of this calculation is highlighted in Figures 2 and 3. These figures show the cumulative distribution of the derived flux contaminations of a sample of WISE objects at two magnitudes – one faint, one bright. Plotted are the $\Delta m = 10$ previous limit, for

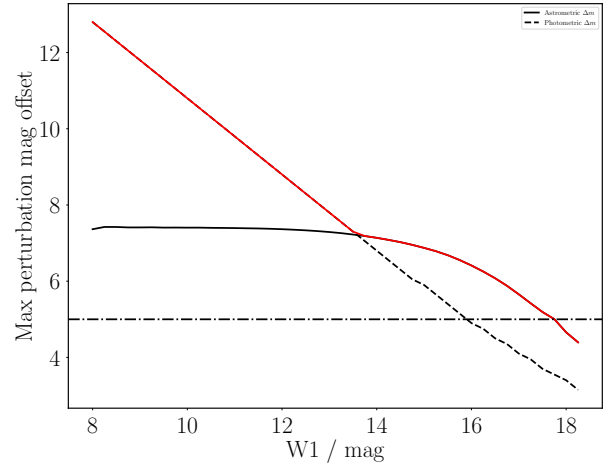


Figure 1. Magnitude offsets for considering blended objects to, for both astrometric and photometric considerations, for WISE sources at $l = 130$, $b = 0$. The Δm for astrometric completeness – the limit at which the secondary object is 5% the noise of the primary object – is shown in solid black. The photometric magnitude offset – the magnitude offset down to which sources must be drawn for 99% of realisations to contain at least one source – is shown in dashed black. The red line shows the maximum of the two; and the dash-dot black line shows $\Delta m = 5$, important for LSST using TRILEGAL simulations.

reference, along with a $\Delta m = 15$ case, representing a “complete” limit at all brightnesses. Also plotted are the astrometric Δm derived previously, and the new photometric limit.

It can be seen in Figure 2 that neither the astrometric limit, nor the original Δm , capture the tail in the distribution of fluxes from sources of $W1 = 9$. These objects are bright, and thus not subject to significant crowding at relative flux ratios that contribute to the overall quoted flux; however, the astrometric limit causes two thirds of cases to be quoted as having zero additional flux. While the individual sources are at $\Delta f \approx 0.001$, we can ensure that our distribution of flux brightenings is robust across all statistics by increasing Δm to 10 or even 12, with little computational cost. This then ensures we track our Δf flux brightenings down to 10^{-5} , providing the full statistical distribution of potential contamination levels, which could be of use.

Figure 3 shows a different story, however. At these fainter magnitudes, the photometric limit – defined as the point at which we draw zero sources no more than 1% of the time – is achieved much quicker, as these sources are much more subject to crowding. Here, the astrometric limit begins to dominate, and we can stop worrying about the photometry, as it can be assumed to be complete at the astrometric limit. Thus, as Figure 1 shows, the photometric limit matters more at bright magnitudes than the astrometric limit, as shown by the handoff between the two at $W1 \approx 14.5$.

We can therefore now derive a Δm which ensures that both the astrometric perturbations and photometric contamination of simulated objects are as accurate as possible. This then allows for robust secondary parameters, such as flux brightening of individual sources subject to crowding in a given photometric catalogue, to be quoted along with likely cross-matches to secondary catalogues. In addition, this method can adjust the acceptable fraction of PSF realisations with zero perturbers y , analogous to the $B = 0.05$ result for astrometric SNR considerations, allowing for flexibility in the derivation of the photometric Δm .

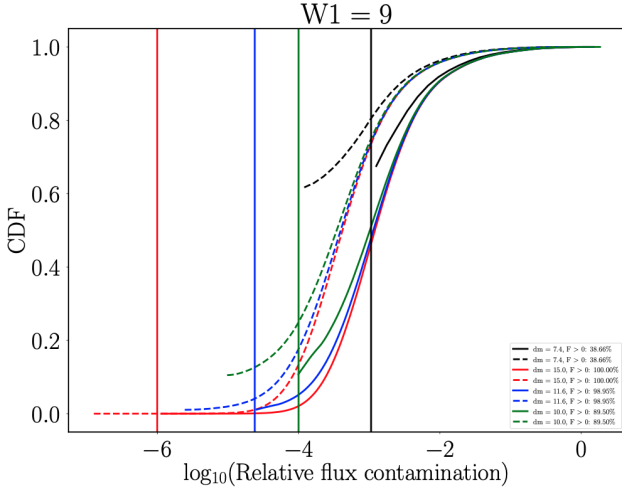


Figure 2. Cumulative distributions of derived flux contaminations from Monte Carlo simulations of blended sources within PSFs, assuming a *WISE* source of $W1 = 9$. Various Δm limits are shown: the previously computed astrometric limit (black line), 15 (red line), the photometric limit (blue line), and 10 (green line). Additionally, the flux contaminations from a simple flux-weighted centroid (solid lines) and the log-likelihood maximisation method (dashed lines) are shown. Vertical lines show the lower limit on f , based on $f = -2.5 \log \Delta m$. CDFs include sources for which zero objects were realised, which is why some CDFs do not begin at zero (i.e., if 40% of objects are “pure”, the CDF would start at 0.4).

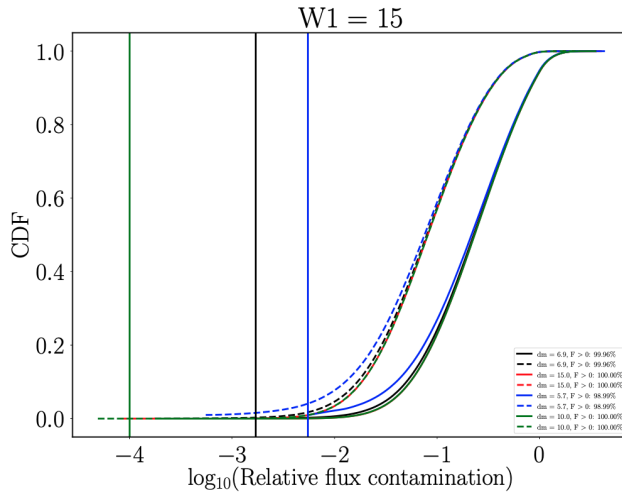


Figure 3. Cumulative distributions of derived flux contaminations from Monte Carlo simulations of blended sources within PSFs, assuming a *WISE* source of $W1 = 15$. Colours and line styles are the same as in Figure 2.

3 FLUX CONTAMINATION COMPUTATIONS AT ALL SIGNAL-TO-NOISE RATIOS

Previously, we derived a new method for computing the astrometric perturbations of sources in the background-dominated, PSF-fit regime, applicable to faint LSST objects. This new algorithm was combined with the previously used flux-weighted centroids in a magnitude-based weighted average scheme (see figure 7, March report, e.g.). However, this left – as detailed in section 4 of the March report – an outstanding question of how to handle PSF-fit sources

at bright magnitudes. We detail here a test into this question, using simulated test image cutouts with realistic *WISE* counts and noise.

3.1 Simulating Crowded PSFs

For a series of *W1* magnitudes, we create small representative images of a single PSF, and add extra sources, representing simulated perturbers. The PSF used is the *WISE* PSF¹, integrated over a pixel, with image cutouts being 13x13 pixels (roughly two $3\sigma_\phi$ radii, to catch the entirety of a perturber placed at its maximum offset). This is implemented using a *PHOTUTILS* *EPSFMODEL*, fit via *ASTROPY*’s *LEVMarLSQFITTER*. We calculate the “flux,” or, more specifically, the DN counts, of an object by $N = 10^{-(m-m_0)/2.5}$, where $m_0 = 20.5$ is the instrumental zero point of the *W1* filter. The background is chosen to be representative of the same region simulated previously – $l = 130$, $b = 0$ – as the average of the quoted DNs of *WISE* objects in the region, $B = 23$ (again, in DN). It is subtracted from the image once the noise has been simulated. Noise in the image is simulated by drawing each pixel from a Poissonian distribution, with a multiplicative factor of $g = 3.2e^-/\text{DN}$, the gain of the system; this is subsequently removed again once the noise is simulated. The *uncertainty* of each pixel is a combination of several sources: the Poissonian noise from the sources and background (correcting for gain), read noise of 3.1DN, the PSF uncertainty array (as provided with the *WISE* PSF), a flatfield uncertainty of 0.15% flux, and a typical quoted “confusion error” of 0.3DN. These uncertainties are combined quadratically, and the inverse standard deviation is provided as a weight to *LEVMarLSQFITTER*. The main source is also randomly placed within the central pixel, to simulate various pixel phases, and then realisations of the given number density of objects, from the *TRILEGAL* simulation used previously, are drawn and placed.

The resulting composite, blended object is then fit with a single PSF, from random starting position and flux; the build up of 50000 realisations is then flipped into a probability density function (PDF) of perturbations and flux contaminations. We also simulate just the central object, with zero contaminants, and fit the resulting distribution of recorded offsets – in both position and flux – to derive statistical, “pure” Gaussian uncertainties. We then analysed the resultant distribution of perturbed source positional offsets and flux brightenings.

3.2 Bright, PSF-Fit Source Contaminations

The astrometric uncertainty functions (AUFs) follow a very similar shape to those seen in the *Gaia-WISE* cross-matches used in the March report and Wilson & Naylor (2018). We cannot directly compare the simulation to the AUFs seen in the *Gaia-WISE* data, unfortunately, as we cannot simulate several systematic astrometric effects, such as pixel-to-coordinate transformations. We can compare, however, the ensemble *WISE* astrometric uncertainties at each magnitude slice to a quadrature sum of the derived “pure” Gaussian uncertainty from the simulations and a systematic uncertainty. This gives good agreement, with a systematic uncertainty of 0.035”, which is a reasonable “missing” uncertainty, suggesting our simulation is robust as an experiment. A comparison of the statistical distribution of perturbations (the perturbation components of the AUF), convolved with this “representative” *WISE* astrometric uncertainty, shows good agreement with the cross-match offsets in

¹ Cutri et al. (2012), 4.4c

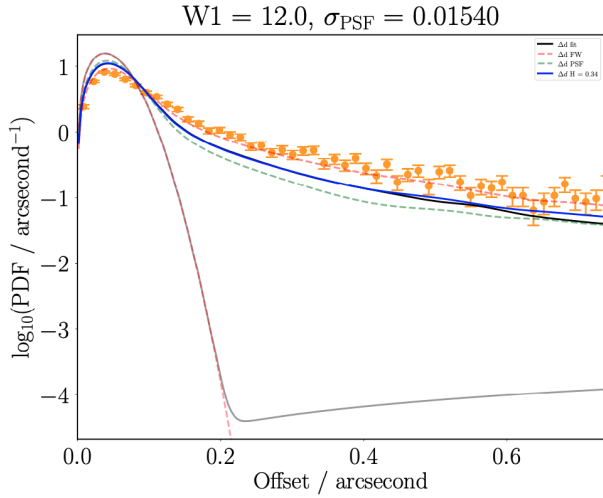


Figure 4. The distribution of perturbations of central object by blended sources. Shown in black are the offsets from “true” of simulated sources, fit via PSF photometry; overlaid in red and green dashed lines are the flux-weighted centroid and background-dominated AUFs, convolved with the intrinsic Gaussian AUF component. Faint black and red lines show simulated “pure” positional offsets, used to derive the intrinsic Gaussian uncertainty, and the intrinsic Gaussian, respectively. The blue line shows the H -weighted AUF; and the orange errorbars show typical *Gaia*-WISE cross-matches for comparison.

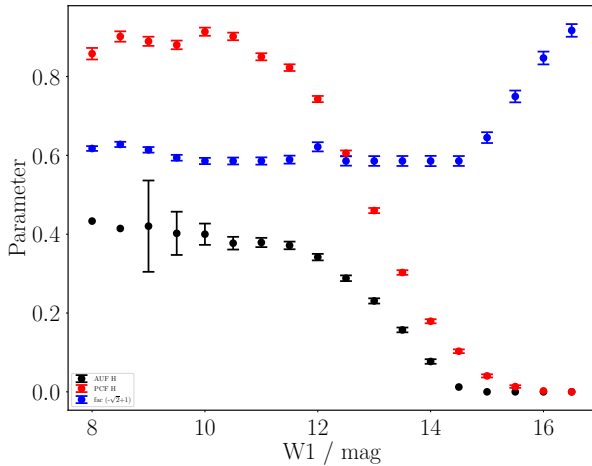


Figure 5. Fit parameters as a function of magnitude for test W1 PSF simulations. Shown are the weighting H between flux-weighted centroid (or aperture photometry flux) and background-dominated perturbations (contaminations) for the AUF (and PCF) in black (and red). Also shown, in blue, is the constant of proportionality between astrometry and photometry, for deriving the relative photometric uncertainty of a given source, offset by $\sqrt{2} - 1$.

the extreme limits of flux. Such an example can be seen in Figure 4, comparing the “flux-weighted” AUF with the *Gaia*-WISE cross-matches shown. This suggests our realisations of perturbing objects are accurate, and thus useful for evaluating the photometric contamination.

The overall trend of H with magnitude for the simulated perturbed positions agrees qualitatively with that seen in the data-driven model; H is larger at bright fluxes, decreasing to zero in the

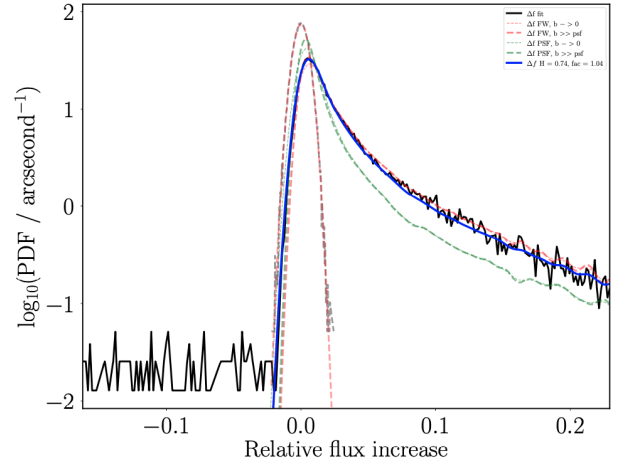


Figure 6. Distribution of photometric contaminations of central object by blended sources. The black line shows the relative flux brightenings of simulated sources, fit via PSF photometry. Faint black and red lines show simulated the “pure” Δf distribution, and its corresponding best fit Gaussian, respectively. The red and green lines show the aperture photometry and background-dominated, PSF-fit flux brightening models, convolved with the “pure” Gaussian noise component, respectively. The dashed and dotted lines (for the red/green lines) show the limits where “fac”, the constant of proportionality between relative astrometric and photometric uncertainties, are 1 (no background) and $\sqrt{2}$ (background-dominated), respectively. The blue line shows the H -weighted PCF, with $1 \leq \text{fac} \leq \sqrt{2}$.

background-dominated case. However, we find that H does not tend to one (shown in Figure 4), as it does with the full *Gaia*-WISE cross-match AUF fits, suggesting some discrepancy in our fits versus the “full” data – an obvious issue being the lack of multi-band fitting. On the other hand, the “ H ” for the photometric contamination function (PCF; the statistical distribution of Δf for a given theoretical source) *does* tend roughly to one at bright magnitudes; the discrepancy here, as with the simulated AUF H , is the magnitude at which H starts to drop. Both H trends for the full magnitude range are shown in Figure 5; see Figure 6 for an example of a PCF fit.

Overall then, there is *reasonable* evidence from these simulations that we can derive a completely analogous function for photometry to that used to compute the astrometric component, the PCF (the photometric “AUF”). We should be able to parameterise the contamination component of the PCF as a piece-meal weighted-average of an aperture photometry model at high SNRs and the model previously derived for background-dominated PSF-fit sources. This can then be convolved with a (now one-dimensional) statistical uncertainty component – albeit with the extra proportionality constant linking astrometric and photometric ratios (see Figure 5, and King 1983 for more details) – to provide a full distribution of potential Δf brightenings.

4 CONCLUSION

In this report we close out the few remaining issues outlined in the March Report for WP deliverable 3.11.1, describing two improvements to the description of sources blended with faint perturbing objects: the photometric simulation limit, and the photometric contamination model.

REFERENCES

- Cutri R. M., et al., 2012, Technical report, Explanatory Supplement to the WISE All-Sky Data Release Products
- Girardi L., Groenewegen M. A. T., Hatziminaoglou E., da Costa L., 2005, [A&A](#), 436, 895
- King I. R., 1983, [PASP](#), 95, 163
- Wilson T. J., Naylor T., 2018, [MNRAS](#), 481, 2148

This paper has been typeset from a $\mathrm{T}_{\mathrm{E}}\mathrm{X}/\mathrm{L}^{\mathrm{A}}\mathrm{T}_{\mathrm{E}}\mathrm{X}$ file prepared by the author.